

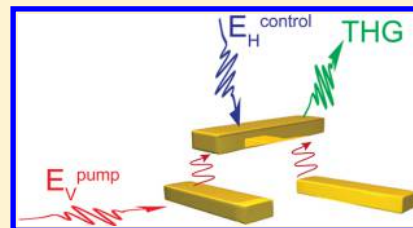
Coupling Mediated Coherent Control of Localized Surface Plasmon Polaritons

Franziska Zeuner,[†] Mulda Muldarisnur,[†] Andre Hildebrandt,[‡] Jens Förstner,[‡] and Thomas Zentgraf^{‡*}

[†]Department of Physics and [‡]Department of Electrical Engineering, University of Paderborn, Warburger Strasse 100, D-33098 Paderborn, Germany

ABSTRACT: We investigate the phase-dependent excitation of localized surface plasmon polaritons in coupled nanorods by using nonlinear spectroscopy. Our design of a coupled three-nanorod structure allows independent excitation with cross-polarized light. Here, we show that the excitation of a particular plasmon mode can be coherently controlled by changing the relative phase of two orthogonally polarized light fields. Furthermore, we observe a phase relation for the excitation that is dominantly caused by damping effects.

KEYWORDS: Plasmonics, coupling, third harmonic generation, coherent control, spectroscopy



Plasmonic nanostructures became an important building block in the field of nanophotonics due to their strong light-matter interactions and the tremendous flexibility in the design of their optical properties for metamaterials and metasurfaces. The plasmonic properties arising from electronic processes at the surface of the metal structures can be ultrafast, highly localized, and therefore potentially interesting for future all-optical computational applications. Such localized electronic excitations, the localized surface plasmon polaritons (LSPP), depend strongly on the structural shape, the surrounding permittivity, and the properties of the metal, providing a high degree of freedom for the design of the optical properties. Metallic nanostructures can also be viewed as plasmonic meta-atoms, that is, elementary building blocks, which preserve atom-like properties like polarizability, resonance behavior and atom-atom-interaction. In addition, the squeezing of optical fields down to a few nanometers can result in a large field enhancement. The field enhancement can be used for a various applications, for example, surface-enhanced Raman-scattering,¹⁻³ enhanced light emission,^{4,5} or nonlinear optical processes.⁶

One of the simplest meta-atoms is a metallic nanorod, which in first approximation behaves like an electric dipole (or dipole nanoantenna).^{7,8} Arrays of such nanoantennas are lately used to build ultrathin metasurfaces with topological phase information to modify the light propagation and realize optical elements such as metalenses⁹ or metaholograms.¹⁰ When plasmonic nanorods are brought very close to each other to form a metamolecule, the LSPP modes of the individual structures can overlap in the near-field and lead to a strong coupling effect, resulting in a hybridization of the original (bare) modes.¹¹ Recently, it was shown that coupled plasmonic nanostructures can be utilized as useful model systems, for example, for classical analogues of electromagnetically induced transparency^{12,13} and absorption.¹⁴ However, for entire control of the optical properties of such nanostructures it is important to gain full control over the plasmonic excitation process, even in more

complex meta-atoms. Here, we demonstrate that the strong near-field coupling among different plasmonic nanorods within a meta-atom unit cell can be utilized to coherently control the excitation of LSPP modes by external light fields.

Although the coupling strength between localized plasmon modes can be controlled via fabrication parameters like distance and arrangement of the nanorods, the active control of the excitation has only been shown for a few cases by controlling phase and amplitude of the excitation fields.^{15,16} It is, however, still very challenging to obtain an all-optical control of LSPP excitations because the short lifetime makes it difficult to control the excitation of a LSPP mode with a pump and a control field directly. The reason is that both fields need to have the same polarization and a short time-delay to avoid direct interference between the two driving pulses.¹⁷ To overcome the problem concerning the short coherence time, the excitation and the control can be decoupled by utilizing two different channels for the excitation process of the same LSPP mode. Here, we propose a technique where the first channel (#1) is a direct excitation by an optical radiation field. LSPPs with sufficiently strong dipole moments can couple strongly to an optical far-field, if the polarization and frequency of the optical field are matching the dipole resonance of the plasmonic nanostructure. The second channel (#2) for the excitation is a near-field coupling to an already excited LSPP mode. However, to obtain a strong coupling and therefore a sufficiently large energy exchange, the modes need to overlap spatially in the near-field. Achieving strong coupling not only requires a close spacing of the mode carrying structures but also a match of the resonance frequency of the modes.¹⁴

In this work, we examine a coupling-induced cancellation of LSPP modes in strongly coupled plasmonic nanostructures. Such a cancellation reflects a coherent control of a localized

Received: April 10, 2015

Revised: May 8, 2015

Published: May 15, 2015

polariton excitation within a particular meta-atom. The structures under investigation consist of an arrangement of three gold nanorods allowing an individual and independent excitation of the LSPP modes for two orthogonal polarized light fields (Figure 1a). We demonstrate that under certain

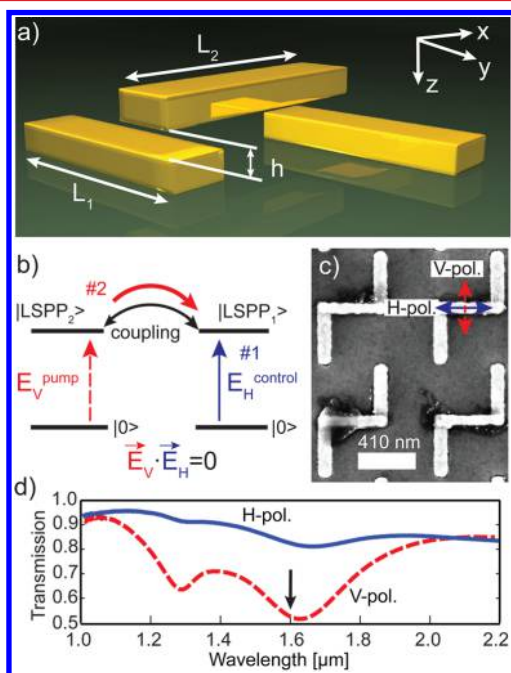


Figure 1. (a) Schematic view of the two-layer coupled structure consisting of three gold nanorods with the relevant geometrical parameters. The lengths of the nanorods are $L_1 = 380$ nm and $L_2 = 410$ nm, respectively. The spacing between the two layers is $h = 30$ nm. (b) Two-level model scheme for controlling the excitation of the bare localized LSPP mode $|\text{LSPP}_1\rangle$ in the upper nanorod via channels #1 and #2. (c) Scanning electron microscopy image of the fabricated structure (top view). Horizontally polarized light (H-pol.) is defined along the single upper nanorod, whereas the electrical field of vertically polarized light (V-pol.) oscillates along the lower nanorods. (d) Polarization dependent transmission spectra measured for H- and V-polarized light. The black arrow marks the wavelength that is used for the experiment to control the excitation of the localized plasmon modes.

excitation conditions the strong coupling among the nanorods can result in a cancellation of the electronic excitation of the coherent conduction band oscillations (antiresonance). This effect is in analogy to a coherent control of the plasmonic excitations by two coherent external light fields.

The plasmonic system shown in Figure 1a possesses two polarization dependent LSPP modes that are represented by orthogonally arranged gold nanorods. This ensures an independent LSPP excitation by orthogonally polarized and therefore noninterfering coherent light fields. To obtain a strong coupling between the nanorods, one rod is stacked closely on top of two further rods, which have the same mode (polarization) orientation. In the following, we are interested in the excitation control of a coherent electron oscillation in the single top nanorod that can be directly excited by an appropriate external light field (with an electric field vector component in x -direction). However, the near-field coupling provides alternative possibility to excite the same LSPP mode in the top nanorod through an external excitation of the two bottom nanorods (which can be excited by y -polarized light

fields). Within the decoherence time of the LSPP (or for long pulse excitation within the coherence time of the two pulses) these two excitation channels can now be used for a coherent superposition of excitation states that is directly controllable by the phase relation between the excitation channels (Figure 1b). Note that this system is similar to the one that has been used to obtain electromagnetically induced absorption in a plasmonic system.¹⁴ However, there a quadrupolar arrangement of the lower dipole wires were used to create a nonradiative “dark mode”. Here, the geometry allows to address both layers of the nanorods independently by orthogonally polarized light since all excitation channels are dipole allowed.

For the experimental investigation of the coupling mechanism, we fabricated gold nanorod arrays with an area of $100 \times 100 \mu\text{m}^2$ by a two-layer electron beam lithography process on a fused silica glass substrate that is covered by a 5 nm-thick ITO layer and a subsequent lift-off processes (Figure 1c). For the metallic nanostructures, we used thermal evaporation of 3 nm chromium and 25 nm gold. After the fabrication of the first layer, a dielectric spin-on glass (Futurrex IC1-200) was spin-coated on the surface followed by a plasma back-etching process to obtain a planar spacer layer between the two nanorod layers. We note that the thickness of this layer will strongly influence the coupling strength and possible retardation effects between the two layers. The dimensions of the fabricated structures are $380 \text{ nm} \times 80 \text{ nm} \times 25 \text{ nm}$ for the lower nanorods and $410 \text{ nm} \times 70 \text{ nm} \times 25 \text{ nm}$ for the upper nanorods. The slightly asymmetric distribution of the dielectric environment of both kinds of nanorods requires a different size in their lengths to match their resonance frequencies. The spacing between the two layers is estimated to be $h = 30$ nm.

The spacing h is a crucial parameter for the near-field mediated coupling, which will not only affect the coupling strength but will also be responsible for retardation effects. Here the configuration of stacked nanostructures was chosen for two reasons: (1) fabricating nanostructures in planar arrangements with only a few nanometers spacing is still challenging, (2) planar arrangements has a smaller mode overlap, consequently the coupling is even weaker. The stacked configuration shows a much larger mode overlap and therefore a stronger coupling.

First, we measured the polarization-dependent linear transmission spectra to obtain the spectral positions of the LSPP modes of the nanorods (Figure 1d). The coupled nanorods show a pronounced normal-mode splitting (two dips in the spectra), which is the result of a hybridization between the modes of the individual dipole wires.^{11,18} Because the number of externally driven dipoles depends on the used polarization, for example, the dips are more pronounced for vertically (V-) polarized light as two nanorods per unit-cell can couple to the driving field. However, the mode-splitting is identical for both excitation geometries as it only depends on the on the coupling strength between the LSPP modes in the nanorods. Like in dolmen-type structures, the lower energy mode at a wavelength of about $1.6 \mu\text{m}$ provides a strong excitation of a coherent electron oscillation in the single top nanorod.¹⁹ This normal LSPP mode is therefore predestined to control an electronic excitation in the top nanorod.

In the following, we will use the low energy mode at $1.6 \mu\text{m}$ for demonstrating the possibility to control the excitation of a coherent electron oscillation. Consider now two driving laser pulses with orthogonal polarizations, which can excite the LSPP mode directly via channel #1 and indirectly through coupling

with the two lower nanorods via channel #2. Then the excitation in the upper nanorod can be extenuated if the excitation phase in channel #1 is out of phase with the excitation via channel #2. On the other hand, a constructive interference due to an in-phase excitation of both excitation paths leads to an enhancement of the excitation process and therefore stronger coherent oscillation of the electrons in the upper nanorod.

Because the injected excitation through channel #2 is much weaker than a direct excitation by the coupling of the external field to the dipole moment through channel #1, the amplitude ratio of both excitation pulses has to be controlled in addition to obtain a high contrast between extenuated and reinforced excitation. Simulations show that an amplitude ratio of 1:1.4 should lead to equal excitation strengths in both channels.

For measuring the strength of the coherent electron excitation in the top nanorod we investigated the third harmonic generation (THG) signal coming from the nanorod. In general, a strong plasmonic excitation corresponds to a large induced current in the nanorods. If the inducing fields are intense and the material/electrons possesses a large non-linearity, the current can provide higher-order contributions to the reemitted fields.²⁰ Hence the large induced currents act as a source of nonlinear optical signals. Because of the orientation of the nanorod and its related strong polarizability along the nanorod, the resulting polarization state of the emitted THG signal will have its main component in the same direction (H-polarized).²¹ The same holds for the bottom two nanorods but with a THG signal that is mainly V-polarized. This opens the possibility to investigate the excitation strength of the upper nanorod by analyzing the H-polarized component of the THG signal from the entire structure. Consequently, constructive and destructive interferences of the excitations lead to an interference pattern of the THG signal if the phase between the two orthogonal excitation pulses (pump and control) is scanned. Therefore, we focus in our experiment on the THG signal coming from the upper nanorod as a function of the relative phase between pump and control field.

The experimental setup for the measurement is sketched in Figure 2a. Within an actively stabilized Michelson-interferometer,²² the laser pulse in one arm is extenuated while in the other arm the polarization of the pulse is changed from horizontal to vertical. With this setup, the relative phase $\alpha = \omega\tau$ between the pump and control pulse (whereas τ is the time delay between the pulses) can be coherently scanned over a wide range, while the second-order cross-correlation function is simultaneously measured via two photon absorption at a silicon photodiode with an additional linear polarizer at the second interferometer exit (Figure 2b). The polarizer is set at an angle under which a minimum of the cross-correlation function corresponds to a π out-of-phase configuration of the pump and control pulses at the sample. After the interferometer, an achromatic lens with $f = 100$ mm focuses the light onto the sample with an array structures oriented like shown in Figure 2a. The peak intensity on the sample is in the order of 0.03 GW/cm², which is about 2 orders of magnitude lower than the expected damage threshold. The THG signal from the sample is collected by a microscope objective (20 \times , NA = 0.45), passed through a short-pass filter (BG39) and a linear polarizer to attenuate the pump wavelength and remove the THG signals with V-polarization coming mainly from the lower nanorods. The signal was then measured by a spectrometer equipped with a cooled CCD detector. Figure 2c shows spectrally resolved

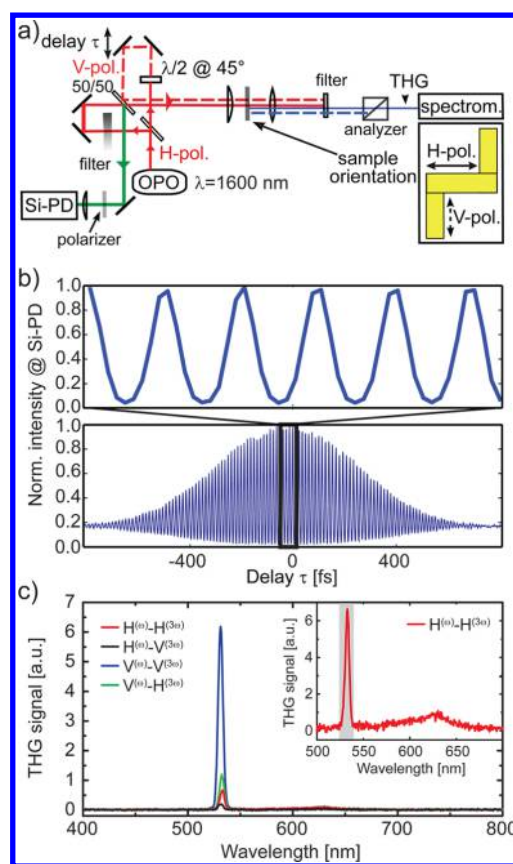


Figure 2. (a) Experimental setup for the investigation of the THG signal from the upper nanorod in dependence of the phase difference between the two excitation pulses. The H-polarized laser pulse is attenuated with a neutral density filter in one arm, while in the other arm the polarization is rotated by 90° to obtain a V-polarized pulse. The first output port of the interferometer is used for exciting the sample while the second port is utilized for monitoring the phase difference between the cross-polarized pulses. (b) Measured second-order cross-correlation function of the two pulses via two photon absorption at a silicon photodiode. For the experiment, only time delays from a small region around the maximum of the cross-correlation function are used where the pulses have the largest time overlap. (c) Measured THG spectra for different polarization states of the fundamental and third-order beams. The measurements are performed for single beam excitation (either H- or V-polarized pulse) with identical intensities. Because of the stronger excitation of the vertical nanorods and the double amount of rods compared to the horizontal nanorods the THG signal is strongest for V-polarized incident fields and V-polarized THG detection. The inset shows a magnified view of the THG spectrum for the case used in the phase-dependent measurements whereas we integrated the THG signal over a range of 16 nm around the center wavelength (shaded area). Because of an additional BG39 filter, the SHG signal at 800 nm from the structure is suppressed.

measurements of the collected sample signal in the range of 400–800 nm for various excitation and detection polarizations and identical illumination intensity. The strong peak at three times (533 nm) of the fundamental frequency (1600 nm) corresponds to the THG from the structures. Despite the THG signal, we do not observe a strong multiphoton luminescence background (e.g., as in ref 23), which is very likely due to the long excitation wavelength and the relatively low excitation intensity in our experiment.

For V-polarized excitation we observe a strong V-polarized THG signal and a five times smaller H-polarized THG component due to the strong coupling to the horizontal nanorod. This component is nearly a factor of 2 stronger as the directly generated H-polarized THG component for H-polarized excitation. Therefore, we attenuated the V-polarized input beam for the phase control experiment to obtain the same THG intensity in the H-polarization state for both excitation polarizations that would result in an equally strong plasmon excitation in the top nanorod and hence in the largest modulation of the THG signal. We note that the cross-polarization terms of the THG signal only come from the coupling effect between the nanorods. For only the lower nanorods without the top rod (no coupling), the THG signal for the H-direction would be forbidden by symmetry.

For the modified intensity ratio between the two excitation polarizations, we measured the H-polarized THG signal intensity in dependence of the relative phase delay α between the pump and probe pulse (Figure 3 top panel). The

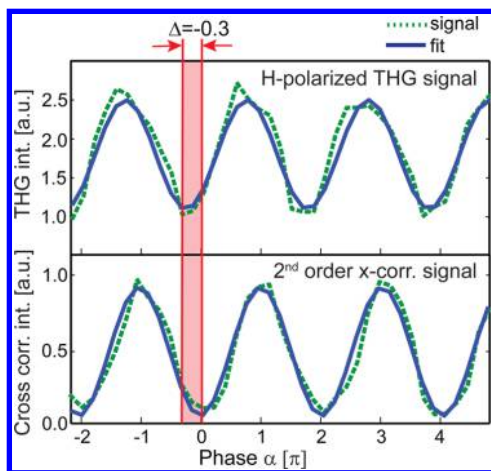


Figure 3. Measured THG signal intensities (top) with respect to phase delays $\alpha = \omega\tau$ between the cross-polarized pump and probe pulses. The signal is compared to the second-order cross-correlation function of the laser pulses (bottom) and exhibits a phase shift of about $\Delta = (-0.3 \pm 0.1)\pi$.

measurement result shows a periodic modulation of the H-polarized THG signal with the relative phase delay between the two pulses. When we fit the THG intensity with a cosine function and compare it to the measured second-order cross-correlation intensity from the Si-photodiode we obtain a phase shift between these two of $\Delta = (-0.3 \pm 0.1)\pi$ for every phase step. The physical origin of the phase delay lies in the resonant behavior of the plasmonic system and can be understood with a classical externally driven damped oscillator model. For a classical oscillator, any driving force applied to the system with driving frequencies near the resonance frequency is 0.5π out of phase compared to the internal oscillation. However, if the driving frequency is shifted away from the resonance frequency of the system the phase shift becomes smaller or larger, depending on the direction of the frequency shift. In our experiment, we operate at the lower frequency side of the original bare LSP resonance, therefore our observed phase shift is smaller than 0.5π . Note that the obtained phase shift has to be seen with respect to the phase defined by the cross-correlation function at the Si-diode, which is determined by the placement angle of the polarizer.

In our interpretation, we assumed that the currents (i.e., the LSPs) act as the source of the nonlinear optical signal coming from the nanorods. Therefore, the current strength should highly correlate with the intensity of the THG signal. To support our interpretation of the experimental results we calculated the spatial current density in x -direction in the upper nanorod (using CST Microwave Studio). For the simulations, two linearly cross-polarized excitation pulses with a given phase difference α are sent onto the structure and the current density J_x is calculated as a function of this phase. The definition of the state with $\alpha = 0$ is chosen to be the same as in the experiment. The simulations were performed for the same structure dimensions as in the experiment. Because of the unknown dispersion of the spin-on-glass and the used simple Drude model for bulk gold the linear transmission of the structure (see inset in Figure 4) is slightly red-shifted compared to the experimental curve. Nevertheless, the qualitative characteristics of a normal mode splitting are represented very well.

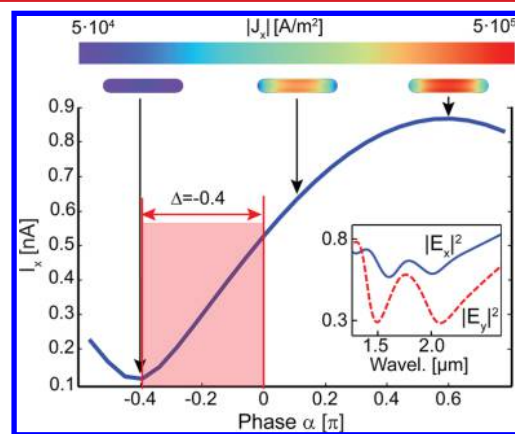


Figure 4. Simulated current in the upper nanorod as a function of the phase α between the two excitation pulses. The simulation shows the smallest current in the nanorod for a phase shift of $\Delta = -0.4\pi$. The cross-section of the spatial current density inside the upper nanorod (2 nm from the top surface) is plotted for three phases. The current density is calculated for an excitation wavelength of $2 \mu\text{m}$. Inlay: linear transmission of the simulated structure for excitations in x - and y -direction showing the normal mode splitting and the different excitation strengths for the two polarizations.

From the simulations we extracted the current density of the lower energy mode in the top nanorod of the structure at $2 \mu\text{m}$, which corresponds approximately to the $1.6 \mu\text{m}$ in the experiment. Figure 4 shows the current calculated from the current density in the nanorod depending on the phase relation α . Note that a phase of $\alpha = 0$ corresponds to an excitation configuration where the orthogonal pump and control fields are in phase. We observe the smallest current in the nanorod for a phase retardation of $\Delta = -0.4\pi$ between the pump and control pulse. For that phase delay we would expect the weakest THG signal from the nanorod in H-polarization, which is in agreement with our experimental observation.

Further simulations show a wavelength-dependent phase shift, which follow the characteristics of a damped resonant system. Interestingly, although the system consists of two coupled oscillators, it behaves like one single resonant system.

In conclusion, we have demonstrated the coherent control of LSPs in a nanorod array. For this purpose, we have investigated the third harmonic signal emitted from nanorods

that were excited via two different channels, namely a near-field coupling channel and a direct far-field excitation channel. Changing the relative phase between these channels results either in a destructive or constructive interference, respectively. The cancellation of the excitation was measured as a minimum of the THG signal. Moreover, we observed a phase shift between the THG signal and the excitation. On the basis of our structure design, we eliminate retardation of the light caused by the spacing as the origin for the phase shift, because its value would only be in the order of a tenth of the observed phase shift. Accompanied with simulations, which reproduce the experimental observations very well, we found that the phase shift is a result of the high damping by ohmic and radiation losses and therefore the short coherence times of the LSPPs in the nanorods. Similar to driven and damped harmonic oscillators close to the resonance, this coupled plasmonic systems also shows a phase shift close to 0.5π for resonant excitation. Our observations open not only the possibility for a coherent control of LSPPs by external light fields but also an all optical control of nonlinear properties on the nanoscale. The results demonstrate that the coupling effect between nanostructures can be utilized to gain more access to a tailored-controlled excitation of localized modes.

AUTHOR INFORMATION

Corresponding Author

*E-mail: thomas.zentgraf@uni-paderborn.de.

Notes

The authors declare no competing financial interest.

ACKNOWLEDGMENTS

This work was partly supported by the European Commission under the Marie Curie Career Integration Program. The authors acknowledge the financial support by the DFG Priority Program SPP1391 “Ultrafast Nanooptics” and the support by the DFG Research Center TRR142 “Tailored nonlinear photonics”.

REFERENCES

- (1) Kneipp, K.; Wang, Y.; Kneipp, H.; Perelman, L. T.; Itzkan, I.; Dasari, R. R.; Feld, M. S. *Phys. Rev. Lett.* **1997**, *78*, 1667–1670.
- (2) Kneipp, K.; Wang, Y.; Kneipp, H.; Itzkan, I.; Dasari, R. R.; Feld, M. S. *Phys. Rev. Lett.* **1996**, *76*, 2444–2447.
- (3) Talley, C. E.; Jackson, J. B.; Oubre, C.; Grady, C.; Hollars, C. W.; Lane, S. M.; Huser, T. R.; Nordlander, P.; Halas, N. J. *Nano Lett.* **2005**, *5*, 1569–1574.
- (4) Kwon, M.-K.; Kim, J.-Y.; Kim, B.-H.; Park, I.-K.; Cho, C.-Y.; Byeon, C. C.; Park, S.-J. *Adv. Mater.* **2008**, *20*, 1253–1257.
- (5) Xiao, X. H.; Ren, F.; Zhou, X. D.; Peng, T. C.; Wu, W.; Peng, X. N.; Yu, X. F.; Jiang, C. Z. *Appl. Phys. Lett.* **2010**, *97*, 071909.
- (6) Kauranen, M.; Zayats, A. V. *Nat. Photonics* **2012**, *6*, 737–748.
- (7) Mühlischlegel, P.; Eisler, H.-J.; Martin, O. J. F.; Hecht, B.; Pohl, D. W. *Science* **2005**, *308*, 1607–1609.
- (8) Ghenuche, P.; Cherukulappurath, S.; Taminiau, T. H.; van Hulst, N. F.; Quidant, R. *Phys. Rev. Lett.* **2008**, *101*, 116805.
- (9) Chen, X.; Huang, L.; Mühlenbernd, H.; Li, G.; Bai, B.; Tan, Q.; Jin, G.; Qiu, C.-W.; Zhang, S.; Zentgraf, T. *Nat. Commun.* **2012**, DOI: 10.1038/ncomms2207.
- (10) Huang, L.; Chen, X.; Mühlenbernd, H.; Zhang, H.; Chen, S.; Bai, B.; Tan, Q.; Jin, G.; Cheah, K.-W.; Qiu, C.-W.; Li, J.; Zentgraf, T.; Zhang, S. *Nat. Commun.* **2012**, DOI: 10.1038/ncomms3808.
- (11) Prodan, E.; Radloff, C.; Halas, N. J.; Nordlander, P. *Science* **2003**, *302*, 419–422.
- (12) Liu, N.; Langguth, L.; Weiss, T.; Kästel, J.; Fleischhauer, M.; Pfau, T.; Giessen, H. *Nat. Mater.* **2009**, *8*, 758–762.

- (13) Zentgraf, T.; Zhang, S.; Oulton, R. F.; Zhang, X. *Phys. Rev. B* **2009**, *80*, 195415.
- (14) Taubert, R.; Hentschel, M.; Kästel, J.; Giessen, H. *Nano Lett.* **2012**, *12*, 1367–1371.
- (15) Stockman, M. I.; Faleev, S. V.; Bergman, D. J. *Phys. Rev. Lett.* **2002**, *88*, 067402.
- (16) Kao, T. S.; Jenkins, S. D.; Ruostekoski, J.; Zheludev, N. I. *Phys. Rev. Lett.* **2011**, *106*, 085501.
- (17) Zentgraf, T.; Christ, A.; Kuhl, J.; Giessen, H. *Phys. Rev. Lett.* **2004**, *93*, 243901.
- (18) Liu, N.; Guo, H.; Fu, L.; Kaiser, S.; Schweizer, H.; Giessen, H. *Adv. Mater.* **2007**, *19*, 3628–3632.
- (19) Ye, Z.; Zhang, S.; Wang, Y.; Park, Y.-S.; Zentgraf, T.; Bartal, G.; Yin, X.; Zhang, X. *Phys. Rev. B* **2012**, *86*, 155148.
- (20) Boyd, R. W. *Nonlinear Optics*, 3rd ed.; Elsevier: New York, 2008.
- (21) Metzger, B.; Schumacher, T.; Hentschel, M.; Lippitz, M.; Giessen, H. *ACS Photonics* **2014**, *1*, 471–476.
- (22) Wehner, M. U.; Ulm, M. H.; Wegener, M. *Opt. Lett.* **1997**, *22*, 1455–1457.
- (23) Rodrigues, S. P.; Lan, S.; Kang, L.; Cui, Y.; Cai, W. *Adv. Mater.* **2014**, *26*, 6157–6162.